Published online 21 March 2018

Nucleic Acids Research, 2018, Vol. 46, No. 11 ***5809–5821***
doi: 10.1093/nar/gky214

Long noncoding RNA OCC-1 suppresses cell growth through destabilizing HuR protein in colorectal cancer

Yang Lan[1], Xuewei Xiao[1], Zhengchi He[1], Yu Luo[1], Chuanfang Wu[1], Ling Li[1] and Xu Song[1,2,*]

[1]Center for Functional Genomics and Bioinformatics, Key Laboratory of Bio-Resource and Eco-Environment of Ministry of Education, College of Life Sciences, Sichuan University, Chengdu 610065, Sichuan, P.R. China and [2]State Key Laboratory of Biotherapy, West China Hospital, Sichuan University, Chengdu 610041, Sichuan, P.R. China

Received August 23, 2017; Revised March 11, 2018; Editorial Decision March 12, 2018; Accepted March 13, 2018

ABSTRACT

Overexpressed in colon carcinoma-1 (OCC-1) is one of the earliest annotated long noncoding RNAs (lncRNAs) in colorectal cancer (CRC); however, its function remains largely unknown. Here, we revealed that OCC-1 plays a tumor suppressive role in CRC. OCC-1 knockdown by RNA interference promotes cell growth both *in vitro* and *in vivo*, which is largely due to its ability to inhibit G0 to G1 and G1 to S phase cell cycle transitions. In addition, overexpression of OCC-1 can suppress cell growth in OCC-1 knockdown cells. OCC-1 exerts its function by binding to and destabilizing HuR (ELAVL1), a cancer-associated RNA binding protein (RBP) which can bind to and stabilize thousands of mRNAs. OCC-1 enhances the binding of ubiquitin E3 ligase β-TrCP1 to HuR and renders HuR susceptible to ubiquitination and degradation, thereby reducing the levels of HuR and its target mRNAs, including the mRNAs directly associated with cancer cell growth. These findings reveal that lncRNA OCC-1 can regulate the levels of a large number of mRNAs at post-transcriptional level through modulating RBP HuR stability.

INTRODUCTION

Long noncoding RNA (lncRNA) is a class of large transcripts (>200 nucleotides) with limited protein-coding potential. Many thousands of lncRNAs are pervasively transcribed from the human genome (1), and dozens of them have been reported to function in both physiological and pathological processes (2,3). LncRNAs play crucial roles in multiple steps of gene regulation by serving as guides of chromatin-modifying complexes (4–6) and transcription factors (7–9), scaffolds of protein-protein interactions (9–11), decoys of proteins (12–14), sponges for miRNAs (15–18), etc. Aberrant expression of lncRNAs is common in cancer (19), and lncRNAs have been found to involve in various aspects of cancer development such as cell growth, survival, invasion and metastasis (5,14,20,21). Although lncRNA has been widely acknowledged as a new contributor to human cancer, only a small number of lncRNAs have been functionally characterized in colorectal cancer (CRC), and most of their mechanisms are largely unknown.

The stability of mRNA is controlled by dozens of RNA-binding proteins (RBPs) (22). Dysregulation of these RBPs, which can lead to aberrant expression of cancer-related genes, has been widely observed in cancer (23). HuR (ELAVL1), the ubiquitous member of the Hu/ELAV (human/embryonic lethal abnormal vision) RBP family, is a positive regulator of RNA stability that has been widely implicated in cancer progression. In the cytoplasm, HuR binds to the AU-rich elements (AREs) in the 3′UTRs of thousands of its target mRNAs (24,25), including numerous mRNAs that are involved in diverse biological processes of carcinogenesis (25). Elevated cytoplasmic HuR protein level has been observed in many types of cancers (26). In CRC, increased HuR protein in cytoplasm associates with advanced tumor (T) stage (27), and importantly, overexpression of HuR increased the growth of colon cancer cells in a nude mouse xenograft model (28). The level of HuR protein was found to be modulated by the ubiquitin-proteasome pathway (29), and β-TrCP1 was shown to be the ubiquitin E3 ligase that targets HuR for degradation (30).

Overexpressed in colon carcinoma-1 (OCC-1) (also known as ADG3 (31)) was first identified as a lncRNA that overexpressed in a subset of colon carcinomas (32). However, the function of OCC-1 in CRC has not been fully investigated yet. Here, we found that OCC-1 suppresses CRC cell growth both *in vitro* and *in vivo*. OCC-1 exerts its function by binding to HuR and enhancing its interaction with the ubiquitin E3 ligase β-TrCP1, which leads to HuR ubiquitination and degradation. The degradation of HuR caused by OCC-1 further reduces the levels of HuR target mRNAs, including the mRNAs directly associated with cancer cell growth.

*To whom correspondence should be addressed. Tel: +86 28 85410032; Fax: +86 28 85418926; Email: xusong@scu.edu.cn

MATERIALS AND METHODS

Gene expression and clinical data

The RNAseq gene expression (HiSeqV2) and clinical data of CRC (COADREAD) were downloaded from The Cancer Genome Atlas (TCGA) hub, UCSC Xena (https://xenabrowser.net/datapages/). The microarray gene expression data (GSE39582) were downloaded from Gene Expression Omnibus (GEO, https://www.ncbi.nlm.nih.gov/geo/query/acc.cgi?acc=GSE39582). The microarray data were based on Affymetrix Human Genome U133 Plus 2.0 Array in which OCC-1 expression was measured by probe 225105_at. Primary tumor samples in these two data sets were used for analysis.

Cell culture

Human CRC cells Caco-2, HCT116, HT-29, RKO, SW480 and SW620 were obtained from the Cell Bank of the Chinese Academy of Sciences (Shanghai, China) and cultured under the conditions recommended by the provider. The human embryonic kidney cell line 293T (HEK-293T) was cultured in DMEM (Gibco) media supplemented with 10% fetal bovine serum (FBS, Excell), 100 U/ml penicillin and 100 μg/ml streptomycin (Hyclone).

Cells were transfected with Lipofectamine 2000 (Invitrogen) following the manufacturer's protocol. For the generation of shRNA lentiviruses, HEK-293T cells were co-transfected with pLKO.1 shRNA vectors (Addgene) and packaging plasmids, psPAX2 and pMD2.G (Addgene). Caco-2 and HCT116 cells were transduced with shRNA lentiviruses for RNA interference or transfected with plasmids for OCC-1 expression. Then, the cells were selected by 1 μg/ml puromycin (Sigma) for 5 days. After selection, cell pools were grown in media without puromycin for 24 h before further analysis or treatment. To inhibit protein synthesis or degradation, cells were treated with either cycloheximide (CHX, 50 μg/ml) for 24 h or MG132 (20 μM) for 6 h along with DMSO vehicle controls.

Plasmid construction

For RNA interference, shRNA expression vectors were generated by annealing and inserting shRNA oligonucleotide pairs into pLKO.1 vector. The target sequences of shRNAs are listed in Supplementary Table S1.

For the expression of OCC-1 RNA, the cDNA sequence containing OCC-1 5′UTR and ORF was synthesized by Genewiz Inc. (Suzhou, China) with a FLAG sequence fused in-frame to the 3′ end of the ORF. The OCC-1 3′UTR cDNA sequence was amplified by PCR from Caco-2 cDNA. The full-length FLAG tagged OCC-1 cDNA (FL) was generated by adapter ligation PCR using above two cDNA fragments as templates. A control vector containing only the ORF-FLAG coding sequence (ORF) was constructed by PCR subcloning. Meanwhile, we also generated a construct expressing a frameshift mutant of FL (FS) in which the G immediately after the initial codon was eliminated by ligation PCR to disrupt the ORF entirely. FL and FS shOCC-1-1-resistant mutants (FL^+ and FS^+) were generated by PCR-mediated transversion mutation of the central three bases CAT to GTA in their shOCC-1-1 target sequences.

For ubiquitination assay, ubiquitin (Ub) and HuR cDNA sequences were also amplified by PCR using Caco-2 cDNA, and HA and FLAG tag sequences were added in-frame to their N-terminal (HA-Ub and FLAG-HuR), respectively. All above cDNAs were cloned into a vector containing a puromycin resistance cassette and were under the control of CMV promoter. The sequences of these cDNAs were verified by Sanger sequencing.

Reverse transcription-quantitative PCR (RT-qPCR)

RNA was extracted using TRIzol reagent (Invitrogen), treated with DNase I (Thermo Scientific) and converted into cDNA using random hexamer primers and RevertAid M-MuLV reverse transcriptase (Thermo Scientific). cDNA was quantified by SYBR green I master mix (FOREGENE) and gene-specific primers (Supplementary Table S2) on the StepOnePlus System (Applied Biosystems). PCR amplification reactions were all run in triplicates for each cDNA sample. For comparison, RNA level was first normalized to GAPDH mRNA, and the relative RNA level was determined by setting controls as 1.

Fluorescent in situ hybridization (FISH)

FISH was conducted using RNAscope Multiplex Fluorescent Reagent Kit v2 (Advanced Cell Diagnostics) according to the manufacturer's recommendations. In brief, Caco-2 and HCT116 cells were cultured on chamber slides (Thermo Scientific) for 24 h, then fixed with 4% paraformaldehyde for 30 min, treated with Hydrogen Peroxide for 10 min and digested with Protease III (1:15) for 10 min. RNAscope probes for OCC-1 was added to the cells and hybridized was carried out at 40°C for 2 h in the HybEZ Oven (Advanced Cell Diagnostics). After a series of signal amplification with AMP 1 to 3, cells were incubated with HRP-C1 and then the signal was developed using TSA Plus Cyanine 3 (red, 1:1500, PerkinElmer). Finally, cells were blocked with HRP Blocker, and nuclear were counterstained with DAPI (blue).

Cell Counting Kit-8 (CCK-8)

Cell proliferation was measured by CCK-8 (Dojindo) according to the manufacturer's instructions. Briefly, Caco-2 and HCT116 cells were seeded in triplicates in 96-well plates at 6000 cells/well. Cell culture media were changed into fresh media containing 10% (v/v) CCK-8 reagent at indicated times. After a 2 h incubation under the culture condition, the absorbance at 450 nm of each well was measured on a microplate reader. The mean value of the wells with media alone was used as background and was subtracted from the absorbances of the wells containing cells.

Ki67 staining

For cultured cells, Ki67 staining was carried out using a Ki67 Cell Proliferation Kit (Sangon Biotech, China) according to the manufacturer's recommendations. In brief, cells were rinsed with phosphate-buffered saline (PBS),

fixed in 4% paraformaldehyde for 20 min, and permeabilized with 0.1% Triton X-100 in 0.1% sodium citrate for 10 min. After blocking with 10% FBS in PBS for 1 h, cells were incubated with a rabbit anti-Ki67 antibody (1:100, Sangon Biotech) overnight at 4°C followed by an incubation with a Cy3-conjugated goat anti-rabbit IgG (red, 1:100, Sangon Biotech) for 1 h. Nuclear were counterstained with DAPI (blue).

For tumors from mice model, Ki67 were detected by standard immunohistochemistry protocols. Slides were deparaffinized, hydrated and boiled in EDTA buffer (pH 9.0) for 2 min for antigen retrieval. After treated with 3% H_2O_2 for 25 min, slides were blocked with 3% BSA for 30 min, and then incubated with a rabbit anti-Ki67 antibody (1:100, GB13030-2, Servicebio, China) overnight at 4°C, followed by an incubation with HRP-conjugated secondary antibody (Servicebio) for 50 min. Then, the signal was developed by in DAB (brown) solution for 5 min and the nuclear were counterstained with hematoxylin (blue).

Colony formation assay

Colony formation assay was performed as previously described (33). Caco-2 and HCT116 cells were seeded at 500 cells/well in 6-well plates and cultured for 12 days. The colonies were fixed with 4% paraformaldehyde for 10 min, stained with 0.1% crystal violet for 5 min and washed twice with PBS. The numbers of colonies containing more than 50 cells were counted.

Fluorescence-activated cell sorting (FACS) analysis

Cell cycle distribution was profiled using propidium iodide (PI) staining followed by FACS analysis. In brief, cells were trypsinized into single cell suspension, rinsed extensively with ice-cold PBS and fixed in ice-cold 70% ethanol for 2 h. Then, the cells were treated with RNase A (100 μg/ml) at 37°C for 30 min, stained with PI (sigma) at 4°C for 30 min and subjected to FACS analysis using a BD cytometer (BD Biosciences). The resultant data were analyzed using FlowJo software (Treestar).

Tumorigenesis in nude mice

BALB/c nude mice (5 weeks old) were housed and maintained under special pathogen-free (SPF) condition. All animal experimental procedures were approved by the Animal Care and Use Committee of Sichuan University. OCC-1 knockdown and control cells were trypsinized into single cell suspension and resuspended in PBS with a concentration of 6×10^6/150 μl for Caco-2 and 2×10^6/150 μl for HCT116 cells. Mice were randomly divided into groups ($n = 6$ for each group) and injected subcutaneously in the right flanks with 150 μl of the cell suspensions. Tumors were measured every 3 days with a slide caliper and tumor volume was calculated by the formula: volume (mm^3) = 0.5 × length × $width^2$. After 27 days, mice were sacrificed and tumors were dissected, photographed and weighted.

Microarray mRNA expression analysis

Global mRNA expression was analyzed by the PrimeView Human Gene Expression Array (Affymetrix). Total RNA was converted into cRNA and labeled with biotin using MessageAmp Premier RNA Amplification Kit (#1792, Ambion) according to the manufacturer's instructions. The fragmented cRNAs were hybridized on the gene chip, and then the chip was washed and stained following the manufacturer's standard protocol. The fluorescent signal was scanned by GeneChip Scanner 3000 (Affymetrix) and converted into digital data (.CEL) using Affymetrix GeneChip Command Console (AGCC) software. The resulting data were preprocessed using Robust Multi-array Average (RMA) (34) algorithm. The fold change (FC) of gene expression in shOCC-1 cells was calculated relative to shCTRL cells. A gene was defined as differentially expressed if its $\log_2|FC| > 0.5$.

Gene ontology (GO) enrichment analysis was performed using clusterProfiler (35), an R/Bioconductor package. We further reduced the redundancy of the enriched GO terms using GOSemSim (36) package, which computes the semantic similarity among GO terms.

Western blot analysis

For detection of endogenous OCC-1 polypeptide in CRC cells, western blot was performed according to the previous report in which the polypeptide was identified (31) using three commercially available primary antibodies (ab83945, ab83948 and ab177759, Abcam) raised against three different regions of human OCC-1 polypeptide.

For detection of other proteins in this study, western blot was performed according to standard methods. In brief, proteins were separated by SDS polyacrylamide gel electrophoresis (SDS-PAGE), transferred onto PVDF membranes (Bio-Rad) and incubated overnight at 4°C with corresponding antibodies: anti-FLAG M2-HRP (1:2000; A8592, Sigma), anti-GAPDH-HRP (1:30000; HRP-60004, proteintech), anti-ACTB (1:5000; 60008-I-Ig, proteintech), anti-HuR (1:1000; ab136542, Abcam) and anti-β-TrCP1 (1:1000; 1B1D2, 37–3400, Thermo Scientific). A HRP-conjugated sheep anti-mouse IgG secondary antibody (1:5000; SA00001-I, proteintech) was used for the detection of ACTB, endogenous HuR and β-TrCP1. The protein signals were detected using ECL chemiluminiscent substrate (FOREGENE).

RNA pull-down assay

RNA pull-down assay was carried out as previously described (11). Briefly, the relative long 918-nucleotide OCC-1 3′UTR RNA was synthesized and labeled with Biotin RNA Labeling Mix (Roche) by *in vitro* transcription. The biotin-labeled RNA (1 μg) was first folded in RNA structure buffer (20 mM Tris–Cl [pH 7.0], 0.2 M KCl and 20 mM $MgCl_2$) and then incubated with Caco-2 whole-cell lysate at 4°C for 1 h with rotation. Caco-2 cell lysate was prepared by briefly sonicating 10 million cells in 1 ml IP buffer (25 mM Tris [pH 7.4], 0.15 M NaCl, 0.5% NP-40, 0.5 mM DTT and 1× complete protease inhibitors [Roche]) supplemented with 100 U/ml RNase Inhibitor (Thermo Scientific). After incubation, RNA-protein complexes were retrieved by streptavidin-coupled T1 beads (Dynabeads), washed five times in IP buffer and eluted in Laemmli buffer.

The binding proteins were separated by SDS–PAGE and visualized by silver staining. Protein bands presented only in the OCC-1 3′UTR sample but not in the EGFP RNA and beads-only controls were excised and identified by liquid chromatography–tandem mass spectrometry (LC–MS/MS).

Immunoprecipitation (IP)

RNA IP (RIP) for HuR protein was performed under native condition without crosslinking. Caco-2 whole-cell lysates were prepared as described in the RNA pull-down assay. 2 μg anti-HuR antibody (ab136542, Abcam) or normal mouse IgG (A7028, Beyotime, China) was incubated with 1 ml cell lysates at 4°C for 4 h with rotation. Immune complexes were retrieved by protein G beads (Dynabeads), washed three times in IP buffer and once in LiCl wash buffer (25 mM Tris [pH 7.4], 0.25 M LiCl, 1% NP-40 and 1% deoxycholate). After an additional final wash in IP buffer, the beads were directly resuspended in TRIzol reagent and subjected to RNA extraction. Then, RT-qPCR analysis was performed and the RNA levels in IP samples were normalized to input samples.

HA-Ub IP for ubiquitination assay was carried out with modifications. Ten million MG132-treated Caco-2 cells co-transfected with HA-Ub and FLAG-HuR expression vectors were directly boiled in 0.2 ml SDS lysis buffer (25 mM Tris [pH 7.4] and 1% SDS) and sonicated to dissolve. After 10 times dilution in IP buffer, the cell lysates were incubated with 5 μg anti-HA antibody (340451, Zen BioScience) or normal rabbit IgG (A7016, Beyotime) overnight at 4°C. The ubiquitinated proteins were retrieved, washed as described above, eluted in Laemmli buffer and subjected to western blot using the anti-FLAG antibody to detect ubiquitinated FLAG-HuR.

Co-IP for HuR and β-TrCP1 was also performed under native condition. Ten million Caco-2 cells were lysated in 0.3 ml IP buffer and incubated with 5 μg anti-HuR antibody (ab136542, Abcam) or 20 μl anti-β-TrCP1 (1B1D2, 37-3400, Thermo Scientific) at 4°C overnight with rotation. After retrieved by protein G beads (Dynabeads), the IP complexes were washed 5 times in IP buffer, eluted in Laemmli buffer and subjected to western blot analysis.

Statistical analysis

All statistical analyses were carried out using SPSS Statistics version 20 (IBM). Data are presented as mean± standard deviation of three independent experiments. Significant difference of means between two groups was determined using two-tailed Student's *t*-test. Fisher's exact test was used to calculate the significance of the enrichment of OCC-1-repressed genes in the HuR consensus targets. $P < 0.05$ was considered statistically significant. $*P < 0.5$ and $**P < 0.01$.

RESULTS

Downregulation of OCC-1 associates with advanced tumor T stage in CRC

To investigate the clinical relevance of OCC-1 in CRC, we first analyzed OCC-1 expression using RNAseq gene expression data from TCGA which contain a large number of CRC samples mainly collected from USA. The result showed that OCC-1 expression is significantly downregulated in the samples with advanced T stage (stage II to IV) compared to carcinoma *in situ* (Tis) and stage I tumors ($P = 0.04$, Figure 1A, *left*). We also analyzed OCC-1 expression using an GEO microarray gene expression dataset (GSE39582) containing another independent group of CRC samples collected from France. In consistent, the level of OCC-1 is significantly lower in the advanced T stage tumors ($P = 0.02$, Figure 1A, *right*). These results indicate that OCC-1 is associated with the early development of CRC.

OCC-1 knockdown promotes CRC cell growth both *in vitro* and *in vivo*

We first assessed the abundance of OCC-1 RNA in six common CRC cell lines by RT-qPCR. The result showed that OCC-1 RNA is abundant in these CRC cells (Supplementary Figure S1A). In addition, OCC-1 is predominantly localized in the cytoplasm of Caco-2 and HCT116 cells as revealed by subcellular fractionation (Supplementary Figure S1B) and RNAscope FISH experiment (Figure 1B). To investigate OCC-1 function, we knocked down OCC-1 by RNA interference using two independent short hairpin RNAs (shRNAs, shOCC-1-1 and -2). OCC-1 RNA level was decreased to 28% and 20% in Caco-2 cells and to 40% and 34% in HCT116 cells, compared to a non-target shRNA control (shCTRL) (Figure 1C). Then, we examined the effect of OCC-1 on cell proliferation by CCK-8 assay. The results showed that OCC-1 knockdown significantly increased cell proliferation in Caco-2 and HCT116 cells compared to their control cells (Figure 1D). The increased proliferation was also confirmed by Ki67 staining as the proportions of Ki67-positive proliferating cells were significantly higher in OCC-1 knockdown cells (Figure 1E and Supplementary Figure S2). The increase of Ki67-positive cells also suggested that more G0 quiescent cells re-entered the cell cycle upon OCC-1 knockdown, since Ki67 is only expressed in active stages but not in G0 quiescent phase of the cell cycle. We further assessed the cell cycle distribution of OCC-1 knockdown Caco-2 cells using FACS analysis. The result showed that the total size of G0 and G1 cell portion was reduced, and cells in S phase were increased, with no significant change in G2/M phase cell compartment, which indicates that knockdown of OCC-1 also promoted G1 to S cell cycle progression (Figure 1F). The decrease of G0 and increase of S phase cells indicated that both G0 to G1 and G1 to S cell cycle transitions were accelerated by OCC-1 knockdown in CRC cells. The continued growth capacity of OCC-1 knockdown cells was also evaluated by colony formation assay. The results showed that the OCC-1 knockdown cells formed more colonies than their control cells (Figure 1G), which further confirmed the suppressive role of OCC-1 in cell growth. Furthermore, Transwell assay was performed to test the effect of OCC-1 on cell migration and invasion. However, no significant change in cell migration and invasion ability was observed upon OCC-1 knockdown in both Caco-2 and HCT1116 cells (Supplementary Figure S3). Together, these results suggest that OCC-1 suppresses cell growth by inhibiting both G0 to G1 and G1 to S phase cell cycle transitions in CRC cells.

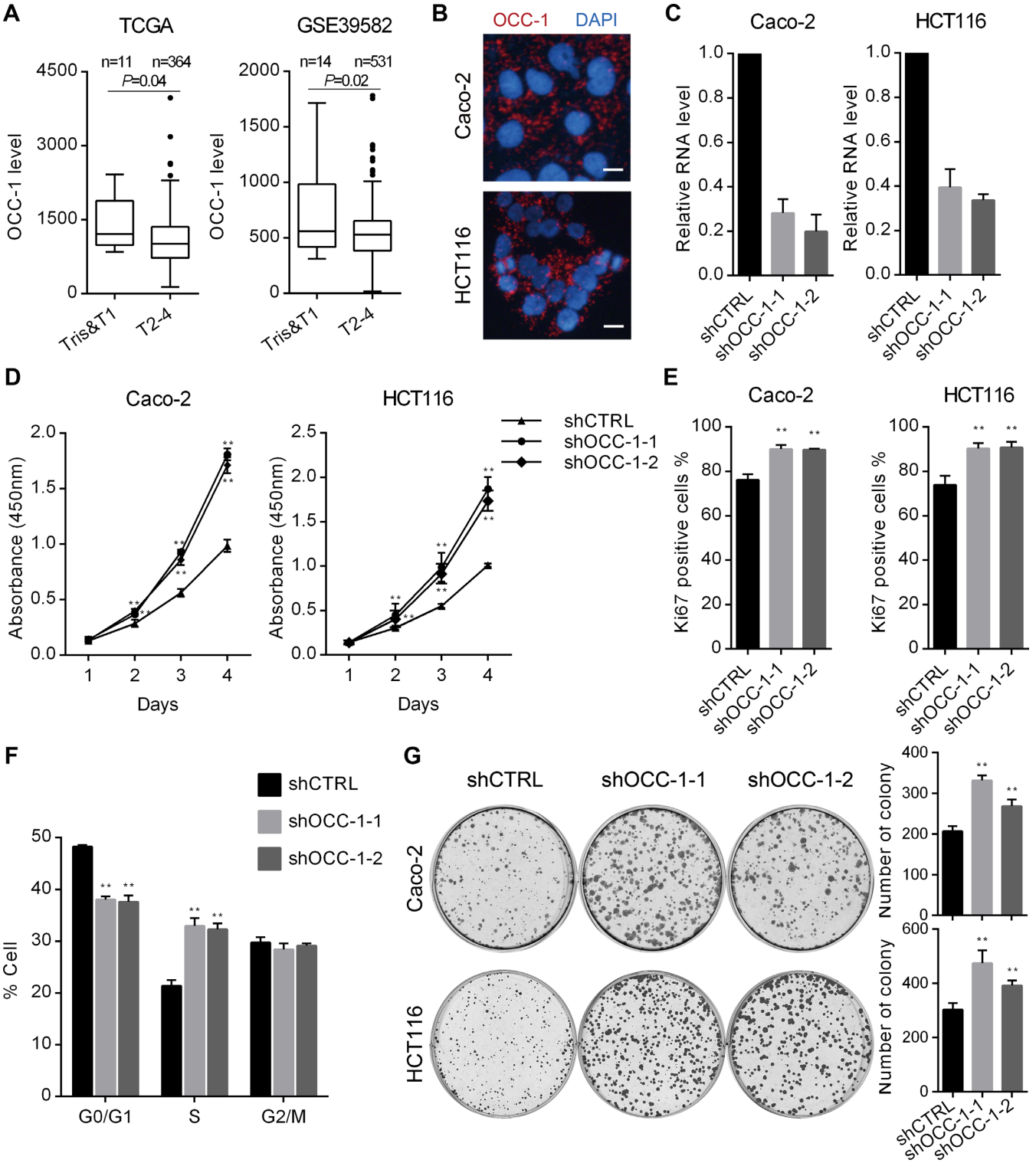

Figure 1. OCC-1 plays a tumor suppressive role in CRC. (**A**) Analysis of two independent gene expression data sets of clinical samples revealed that OCC-1 expression was significantly downregulated in tumors with advanced tumor (T) stage in CRC. Tis, carcinoma *in situ*. (**B**) RNA FISH revealed that OCC-1 is predominantly localized in the cytoplasm of Caco-2 and HCT116 cells (Scale bar, 20 μm). (**C**) RT-qPCR analysis showed that OCC-1 RNA level was efficiently reduced by two independent shRNAs in Caco-2 and HCT116 cells. shCTRL, a non-target shRNA control. (**D**) CCK-8 assay demonstrated that cell proliferation was significantly increased after knockdown of OCC-1 in Caco-2 and HCT116 cells. (**E**) Ki67 staining showed that the proportions of Ki67-positive proliferating cells were significantly higher in OCC-1 knockdown cells compared to their control cells. (**F**) FACS analysis revealed the cell cycle distribution of Caco-2 cells after OCC-1 knockdown. (**G**) Colony formation assay showed that OCC-1 knockdown cells formed more colonies than the control cells. Images are the result of one representative experiment. Data are presented as mean± standard deviation of three independent experiments. $^{**}P < 0.01$.

To test the effect of OCC-1 on cell growth *in vivo*, we performed tumorigenesis assay by subcutaneous injection of OCC-1 knockdown and control cells into the right flanks of nude mice. In the course of tumor development, the volumes of the tumors were measured every 3 days from day 6 after injection and the result showed that tumor growth was accelerated by OCC-1 knockdown in both Caco-2 and HCT116 cells (Figure 2A and B). At 27 days post-injection, tumors were dissected, photographed (Figure 2C) and weighted (Figure 2D). Tumors generated by OCC-1 knockdown cells were significantly bigger and heavier than the tumors of control cells. In addition, cell viability was also increased in the tumors of OCC-1 knockdown cells as determined by Ki67 staining (Figure 2E). These results indicate that OCC-1 also promotes CRC cell growth *in vivo*.

Overexpression of OCC-1 RNA suppresses cell growth in OCC-1 knockdown cells

OCC-1 was found to encode a small polypeptide with unknown function in human bone marrow-derived mesenchymal stem cells (hMSCs) (31); however, we did not detect specific endogenous OCC-1 polypeptide in six common CRC cell lines by western blot using three different commercially available antibodies (data not shown), which is consistent with the initial observation in TC7 CRC cells (32). We constructed a plasmid that expresses a full-length OCC-1 RNA with a FLAG tag fused in-frame to the C-terminal of its potential ORF (FL), a plasmid containing only the ORF-FLAG coding sequence (ORF) and a plasmid expressing a frameshift mutant of FL (FS) in which the ORF is disrupted. When expressed in Caco-2 and HCT116 cells, these three constructs resulted in a similar level of OCC-1 RNAs that were dozens of times higher than that of endogenous OCC-1 (Supplementary Figure S4A and S4B, *left*). However, in comparison to the strong signal of the protein product of OCC-1 ORF, FL yielded a faint protein band that was only detectable through over-exposure in western blot experiments using a high affinity anti-FLAG antibody (Supplementary Figure S4A and S4B, *right*). These results indicate that the endogenous OCC-1 polypeptide, if presents in CRC cells, is expressed at an extreme low level.

To test whether OCC-1 RNA could function as a lncRNA, we further generated two vectors that express the shOCC-1-1-resistant forms of OCC-1 FL and FS RNA (FL^+ and FS^+) by transversion mutation of the central three bases of the shOCC-1-1 target sequences located in their 3′UTR. When transfected into shOCC-1-1 Caco-2 cells, OCC-1 FL^+ and FS^+ were successfully expressed to a level similar to that of OCC-1 ORF, which lacks the whole 3′UTR sequence (Figure 3A). Similar to OCC-1 FL^+, OCC-1 FS^+, the full-length RNA with disrupted ORF, significantly decreased cell proliferation compared to the empty vector (EV) control in OCC-1 knockdown cells as determined by CCK-8 assay, but OCC-1 ORF, which contains only the ORF sequence that produces OCC-1 polypeptide, had no obvious effect on cell proliferation (Figure 3B). Meanwhile, the increase of G0/G1 to S phase transition of OCC-1 knockdown cells was also attenuated by OCC-1 FL^+ and FS^+, with no inhibitory effect of OCC-1 ORF was observed in FACS analysis (Figure 3C). Similarly, reintroduction of OCC-1 RNA by FL^+ and FS^+, but not the polypeptide by ORF, reduced the number of cell colonies formed by OCC-1 knockdown cells in colony formation assay (Figure 3D). Together, these results demonstrated that OCC-1 can suppress cell growth by acting as a lncRNA in CRC cells.

OCC-1 represses the expression of genes involved in cell growth

To gain insight into the molecular function of OCC-1, we profiled the gene expression of Caco-2 cells after OCC-1 knockdown by microarray. The fold change (FC) of gene expression was calculated relative to the control cells, and genes with $\log_2|FC| > 0.5$ were considered as differentially expressed. The two independent shRNAs, shOCC-1-1 and -2, exhibited similar effect on the gene expression profile, with ∼68% and ∼73% differentially expressed genes (DEGs) overlapped with each other (Figure 4A). In total, the expression of 592 genes was disrupted by both shRNAs, and the majority (93%, 554/592) were upregulated, while only 38 genes were downregulated (Figure 4B). The fold changes of the DEGs were modest in the OCC-1 knockdown cells, ranging from 0.41 to 2.3. Gene ontology (GO) enrichment analysis of OCC-1-repressed genes revealed that OCC-1 mainly represses regulators of gene expression that function at post-transcriptional and translational level, particularly these associated with RNA splicing and transport (Figure 4C). We selected several OCC-1-repressed genes that have been reported to be involved in cancer progression and validated their expression by RT-qPCR. Consistent with the microarray analysis, the result confirmed that the levels of these selected genes were all modestly increased after OCC-1 knockdown (Figure 4D). Therefore, we supposed that the upregulation of these cell growth-associated genes is directly responsible for the increased cell proliferation and growth observed in the OCC-1 knockdown cells.

OCC-1 RNA associates with HuR protein

To explore the noncoding function of OCC-1 in gene expression regulation, we performed RNA pull-down assay using OCC-1 3'UTR as RNA probe to identify its protein partner. HuR, a RBP that positively regulates mRNA stability, was identified and the specific binding was verified by western blot (Figure 5A). Furthermore, the association between HuR and OCC-1 was also confirmed in Caco-2 cells by RIP experiment (Figure 5B). In a recent study mapping HuR-binding sites using PAR-CLIP (photoactivatable ribonucleoside enhanced crosslinking and immunoprecipitation), OCC-1 was also found to interact with HuR, with all four CLIP HuR-binding sites localized in its 3′UTR (Figure 5C) (25). The 3′UTR of human OCC-1 contains numerous *in vivo* HuR-binding motifs which has been defined as a stretch of three to four Us flanked by an A or C (37). Moreover, in comparison with other mammals, there are more HuR-binding motifs in OCC-1 3′UTRs in primates, and their distribution tends to be concentrated (Figure 5C), indicating that the binding capacity of OCC-1 to HuR may under positive selection during evolution.

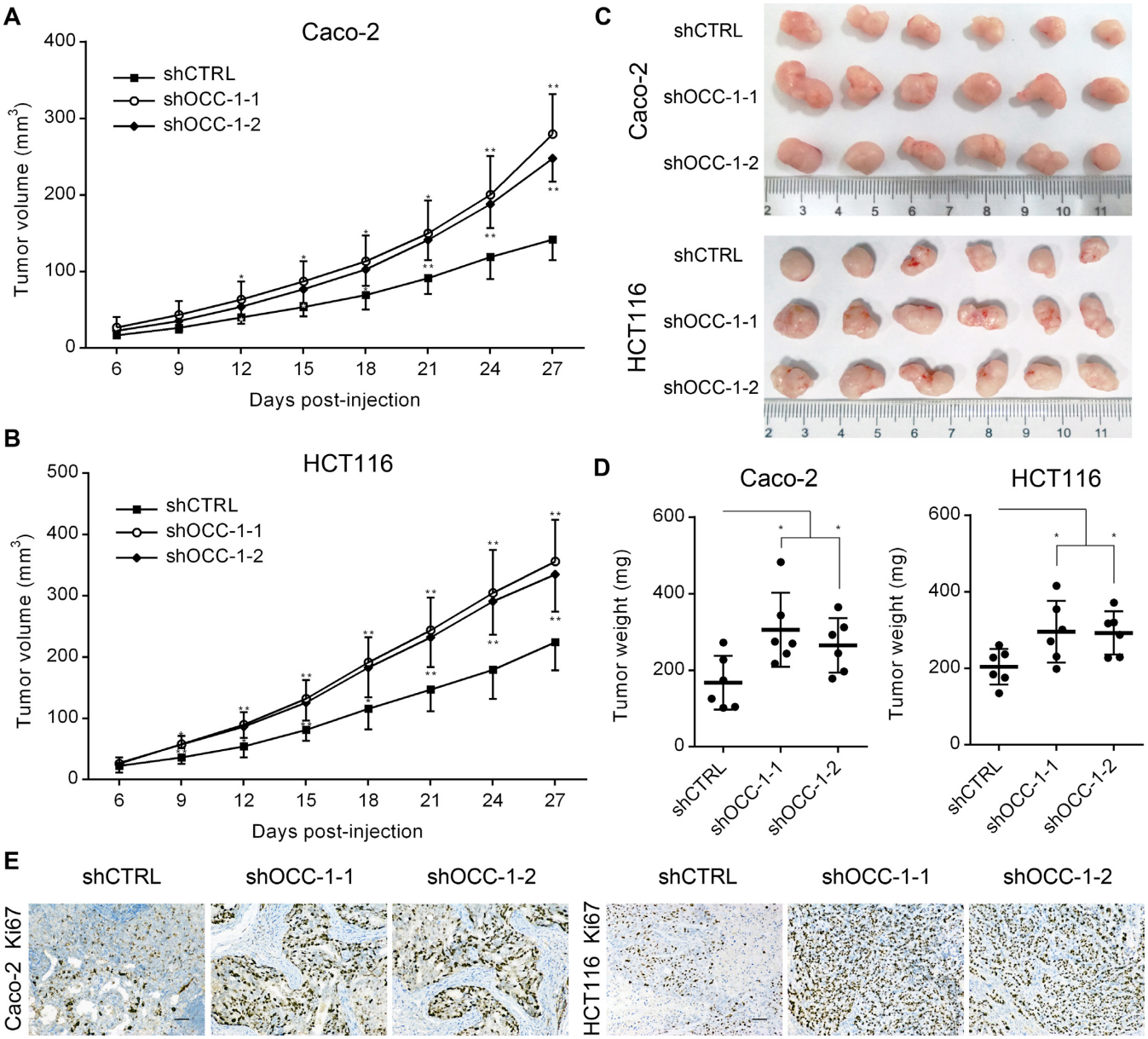

Figure 2. OCC-1 knockdown promoted CRC cell growth *in vivo*. Tumorigenesis assay was performed by subcutaneous injection of OCC-1 knockdown cells into flanks of BALB/c nude mice. (**A** and **B**) Tumor volumes were measured at the indicated days post-injection and tumors were dissected, (**C**) photographed and (**D**) weighted at 27 days post-injection. (**E**) Ki67 staining showed that cell viability was increased in the tumors of OCC-1 knockdown cell (Scale bar, 100 μm). Data are presented as the mean± standard deviation. $n = 6$ for each group. $^{*}P < 0.05$ and $^{**}P < 0.01$.

The CLIP study also defined a set of HuR consensus target mRNAs (25). Similar to the OCC-1-repressed genes detected by our microarray analysis, most of these HuR targets are mRNAs of gene expression regulators that function at post-transcriptional and translational level. Indeed, we found that the OCC-1-repressed genes are significantly enriched for that set of HuR targets ($P < 0.01$), with ∼74% (408/554) of OCC-1-repressed genes are also HuR targets (Figure 5D), including all these six cancer-related genes that have been selected for RT-qPCR validation. Thus, we further examined whether these mRNAs interact with HuR in Caco-2 cells by RIP assay. As expected, the result showed that all these six selected mRNAs were significantly enriched by HuR IP (Figure 5E), suggesting that they are HuR target mRNAs in Caco-2 cells. Then, the effects of HuR on these mRNAs were also tested by knockdown of HuR using a previously validated shRNA, which caused a remarkable decrease in both HuR mRNA and protein level in Caco-2 cells (Figure 5F). The levels of these mRNAs were all slightly but significantly reduced after HuR knockdown (Figure 5G). Together, these results indicate that most of OCC-1-repressed genes are HuR targets, and OCC-1 could downregulate these mRNAs possibly through its association with HuR protein.

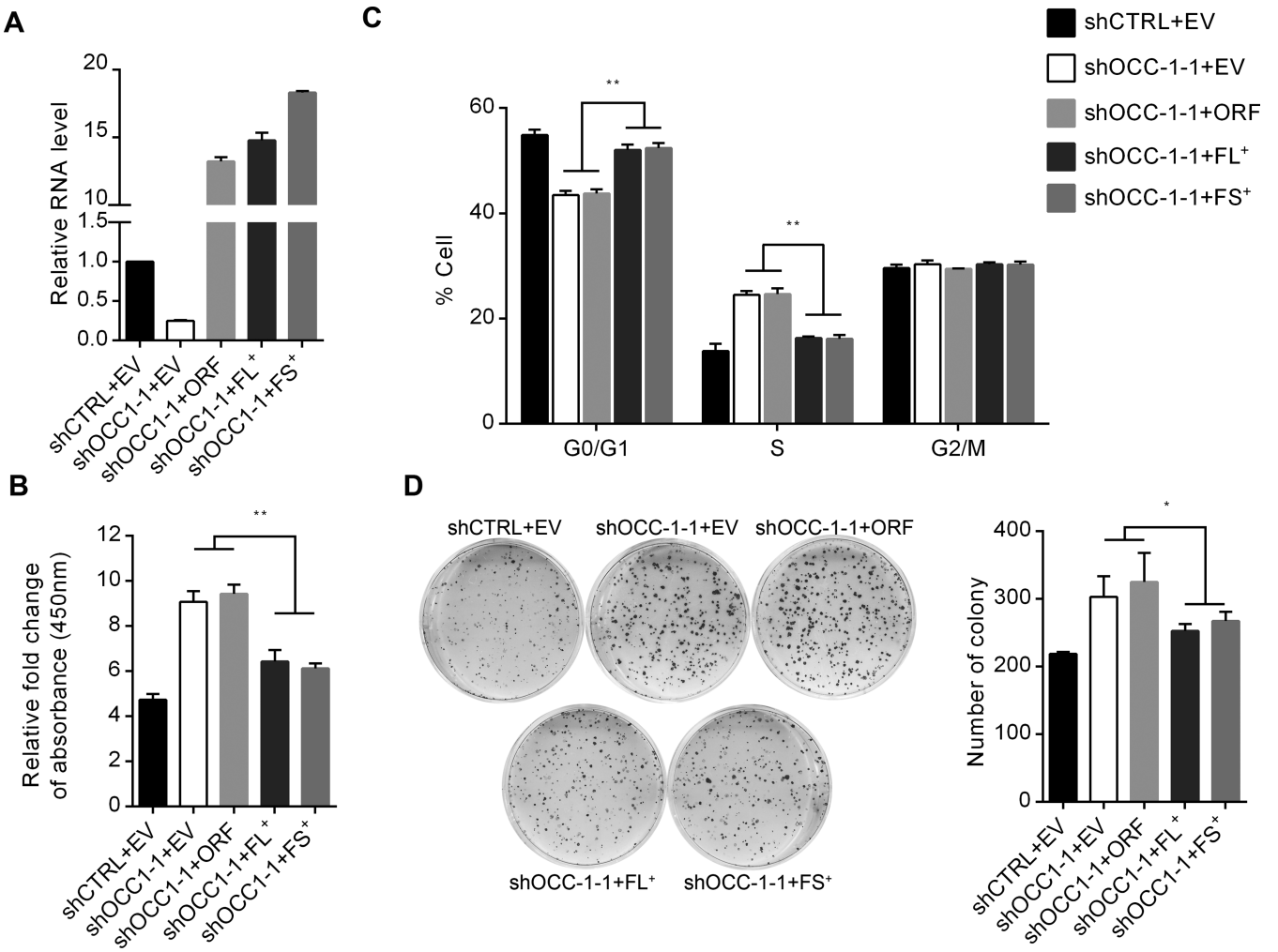

Figure 3. Overxpression of OCC-1 RNA suppressed cell growth in OCC-1 knockdown cells. (**A**) RT-qPCR analysis showed that the shOCC-1-1-resistant forms of OCC-1 FL and FS RNA (FL^+ and FS^+) were successfully overexpressed in shOCC-1-1 Caco-2 cells. EV, empty vector. (**B**) CCK-8 assay demonstrated that cell proliferation was significantly suppressed by the expression of OCC-1 FL^+ and FS^+ RNA but not by the ORF in shOCC-1-1 Caco-2 cells. The fold changes of absorbances at day 4 relative to day 1 were shown. (**C**) FACS analysis revealed the cell cycle distribution of shOCC-1-1 Caco-2 cells after re-introduction of OCC-1 RNAs. (**D**) Colony formation assay showed that the shOCC-1-1 Caco-2 cells expressing OCC-1 FL^+ and FS^+ RNA formed less colonies than the shOCC-1-1 cells expressing the ORF and the EV control. Images are the result of one representative experiment. Data are presented as mean± standard deviation of three independent experiments. *$P < 0.05$ and **$P < 0.01$.

OCC-1 promotes the ubiquitination and degradation of HuR by enhancing its binding to the ubiquitin E3 ligase β-TrCP1

Given the predominant effect of OCC-1 on HuR target mRNAs, we reasoned that OCC-1 may exert its function through regulating HuR protein. Thus, we first determined the effect of OCC-1 knockdown on HuR mRNA and protein level in Caco-2 cells. In consistence with the result of microarray analysis, OCC-1 knockdown had no evident effect on the HuR mRNA level as determined by RT-qPCR (Supplementary Figure S5); however, the level of HuR protein was increased upon OCC-1 knockdown (Figure 6A). In contrast, overexpression of OCC-1-FL^+ and -FS^+ lowers HuR protein level in OCC-1 knockdown cells, while no obvious influence of OCC-1 ORF on HuR protein was observed (Figure 6B). These results indicate that OCC-1 RNA could downregulate HuR protein, and this function is mediated by the RNA itself but not dependent on the polypeptide product.

Given that the level of HuR protein was modulated, we supposed that OCC-1 may regulate the stability of HuR protein. Thus, we treated cells with cycloheximide (CHX) to inhibit protein synthesis and determined the level of remaining HuR by western blot. The portions of HuR remained in OCC-1 knockdown cells were relative higher than in the control cells (Figure 6C), suggesting that HuR protein is more stable upon OCC-1 knockdown. As HuR stability was previously reported to be regulated by the ubiquitin-proteasome pathway (29), we treated the OCC-1 knockdown cells with MG132, a specific proteasome inhibitor, to block the degradation of proteins through proteasome. MG132 treatment resulted in the accumulation of HuR in OCC-1 knockdown cells to the level comparable to that of the control cells (Figure 6D), which demonstrated that HuR is a proteasome substrate, and the relative higher level of

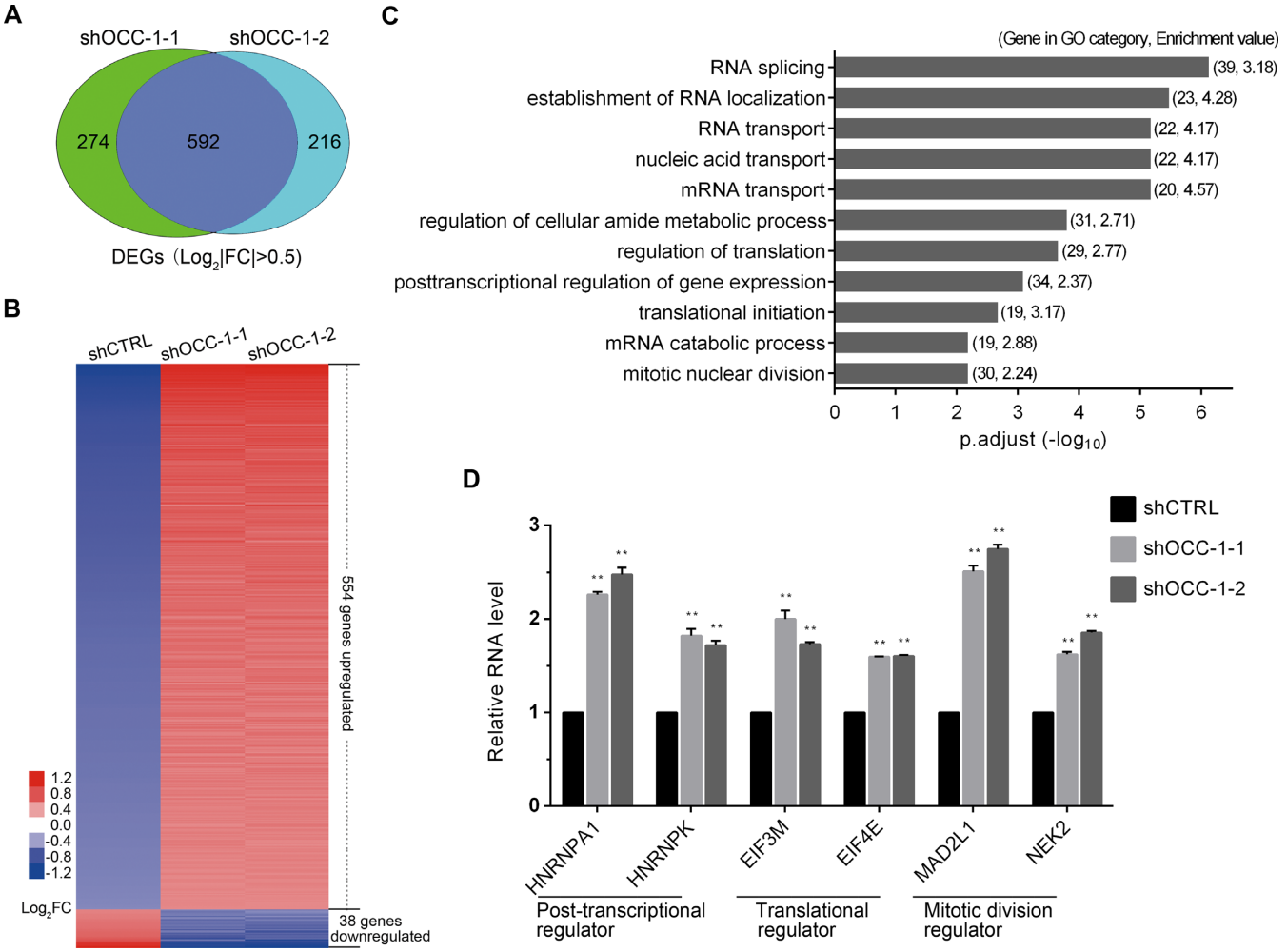

Figure 4. Knockdown of OCC-1 increased the expression of genes involved in cell growth in Caco-2 cells. (**A**) Venn diagram showing that the differentially expressed genes (DEGs) of these two OCC-1 shRNAs identified by microarray were largely overlapped. (**B**) A heat-map showing the 592 DEGs in Caco-2 cells, with most of the DEGs (93%, 554) were upregulated upon OCC-1 knockdown. (**C**) Gene ontology (GO) enrichment analysis of the 521 GO annotated OCC-1-repressed genes revealed that OCC-1 mainly represses the expression of post-transcriptional and translational regulators in gene expression. (**D**) RT-qPCR validation of the expression changes of several OCC-1-repressed genes that have been implicated in cancer cell growth. Data are presented as mean± standard deviation of three independent experiments. $^{**}P < 0.01$.

HuR in untreated OCC-1 knockdown cells is largely due to the reduction of HuR degradation.

We then measured the ubiquitination of HuR in the OCC-1 knockdown cells co-transfected with a plasmid expressing a HA-tagged ubiquitin (HA-Ub) and a plasmid expressing a FLAG-tagged HuR (FLAG-HuR). The ubiquitinated FLAG-HuR protein was captured by HA IP and detected by western blot using an anti-FLAG antibody. The extent of HuR ubiquitination was reduced markedly in the OCC-1 knockdown cells (Figure 6E), which suggests a positive regulatory role of OCC-1 in the process of HuR ubiquitination. Therefore, we further determined the effect of OCC-1 on the binding of HuR to its ubiquitin E3 ligase β-TrCP1, which targets HuR for ubiquitination and degradation (30). Co-IP experiments showed that knockdown of OCC-1 attenuated the interaction between HuR and β-TrCP1 (Figure 6F). Thus, OCC-1 could promote HuR ubiquitination by enhancing the interaction between HuR and E3 ligase β-TrCP1. Together, we reasoned that OCC-1 promotes the ubiquitination and degradation of HuR by enhancing its binding to the ubiquitin E3 ligase β-TrCP1.

DISCUSSION

LncRNA can have oncogenic or tumor suppressive function. In present study, we revealed that OCC-1 suppresses cell growth both *in vitro* and *in vivo* in CRC. OCC-1 binds to HuR protein and renders HuR susceptible to ubiquitination and degradation, thereby reducing the levels of HuR and its target mRNAs, including the mRNAs that associate with cancer cell growth. We reasoned that OCC-1 exerts its function primarily by modulating HuR protein, as ∼74% of OCC-1-repressed mRNAs are known HuR targets (Figure 5D).

OCC-1 was initially identified as a lncRNA in CRC cells (32), but a polypeptide encoded by OCC-1 was observed in hMSCs with unknown function (31). In this study, we also did not detect the endogenous OCC-1 polypeptide in six common CRC cell lines with abundant OCC-1 RNA (data

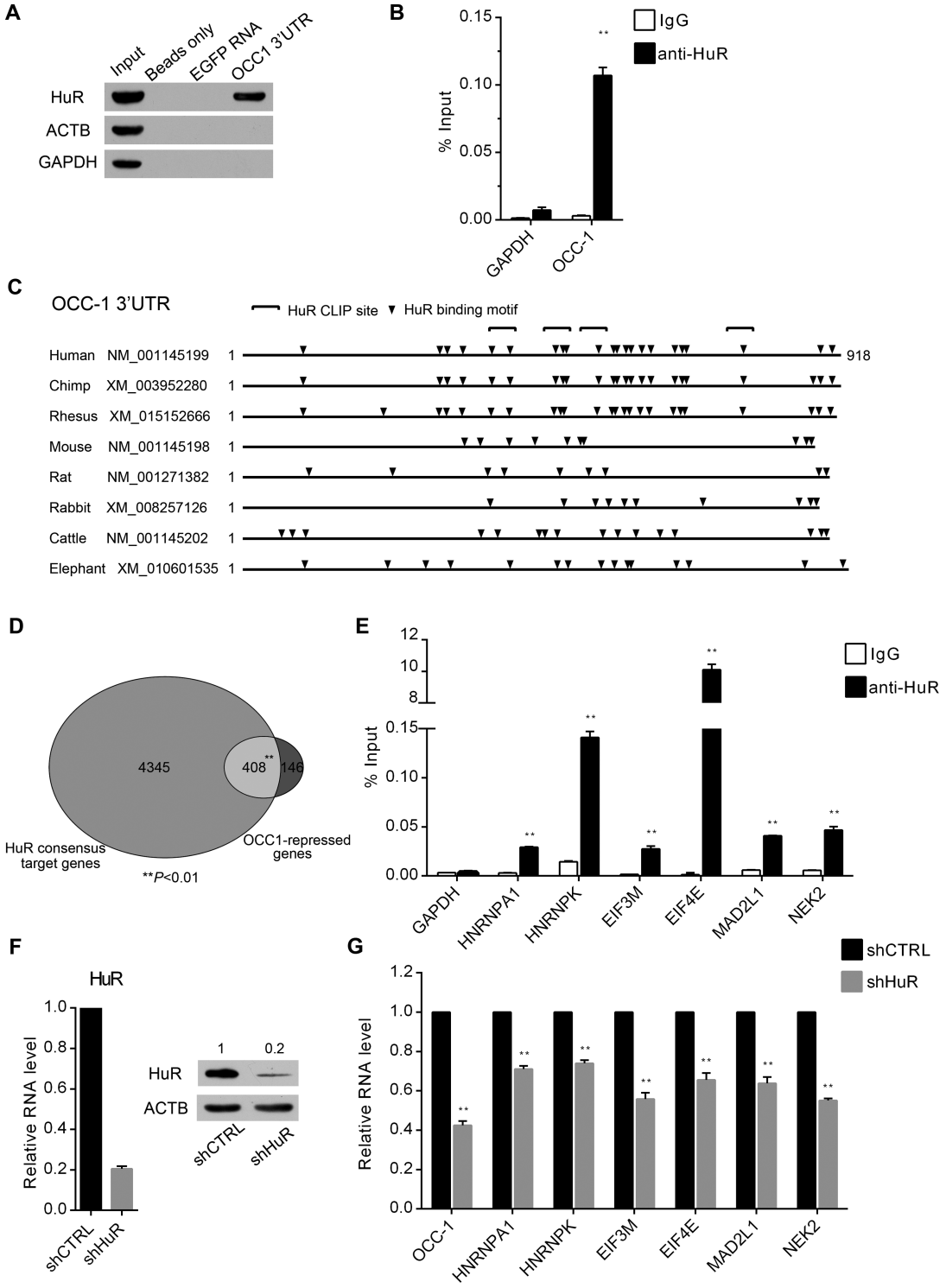

Figure 5. OCC-1 RNA associates with HuR protein. (**A**) RNA pull-down assay followed by western blot confirmed HuR as a protein partner binding specifically to OCC-1 3′UTR. EGFP RNA was used as a RNA control. ACTB and GAPDH are protein controls. (**B**) RIP confirmed the association between OCC-1 and HuR in Caco-2 cells. GAPDH mRNA was used as a non-HuR target control. (**C**) Schematic of the 3′UTRs of OCC-1 orthologues showing the HuR-binding motifs. The HuR-binding sites (HuR CLIP site) identified previously by a CLIP experiment in human OCC-1 3′UTR were also indicated. (**D**) Venn diagram demonstrating the significant enrichment of OCC-1-repressed genes in the set of HuR targets determined by the previous CLIP experiment. About 74% of OCC-1-repressed genes identified by microarray analysis were also HuR targets. (**E**) RIP assay revealed that the mRNAs of the six selected OCC-1-repressed genes also interact with HuR in Caco-2 cells. (**F**) The mRNA and protein level of HuR were markedly reduced by a HuR-targeting shRNA as determined by RT-qPCR (*left*) and western blot (*right*). The density of protein bands was measured by Image J software and the relative level of HuR protein was calculated after normalizing to ACTB protein. (**G**) RT-qPCR analysis revealed that OCC-1 and all six selected OCC-1-repressed genes were downregulated by HuR knockdown. Images are the result of one representative experiment. Data are presented as mean± standard deviation of three independent experiments. $^{**}P < 0.01$.

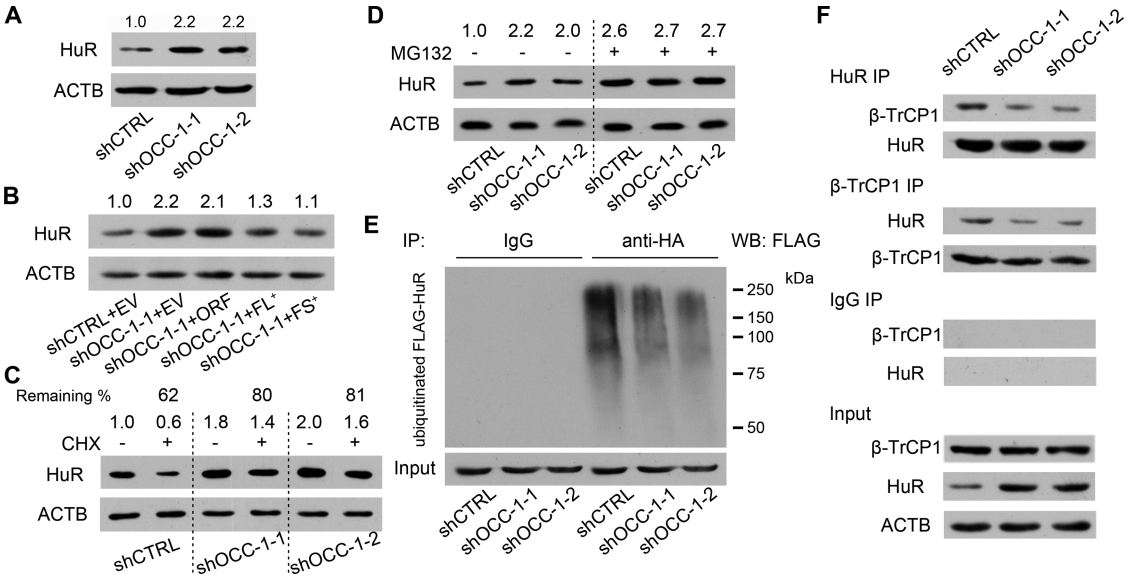

Figure 6. OCC-1 promotes the ubiquitination and degradation of HuR by enhancing its binding to the ubiquitin E3 ligase β-TrCP1. (**A**) Western blot analysis showed that knockdown of OCC-1 led to the increase of HuR in Caco-2 cells. (**B**) Overxpression of OCC-1 FL^+ and FS^+ RNA but not the ORF reduced HuR level in shOCC-1-1 Caco-2 cells. EV, empty vector. (**C**) Cells were treated with CHX to inhibit protein synthesis and the remaining of HuR was measured by western blot in Caco-2 cells after OCC-1 knockdown. The percent of remaining HuR in the CHX treated cells (+) relative to the control cells treated with DMSO (–) was indicated. (**D**) Western blot analysis of HuR in the OCC-1 knockdown cells treated with MG132 (+) or DMSO (–). The density of protein bands was measured by Image J software and the relative level of HuR protein was calculated after normalizing to ACTB protein. (**E**) The OCC-1 knockdown cells were co-transfected with a plasmid expressing a HA-tagged ubiquitin (HA-Ub) and a plasmid expressing a FLAG-tagged HuR (FLAG-HuR). After MG132 treatment, cell lysates were prepared and subjected to IP using an anti-HA antibody. The ubiquitinated FLAG-HuR was further detected by western blot using an anti-FLAG antibody. (**F**) Co-IP experiments showed that the interaction between HuR and the ubiquitin E3 ligase β-TrCP1 was attenuated after OCC-1 knockdown in Caco-2 cells.

not shown). Meanwhile, overexpression of the full-length OCC-1 RNA with a FLAG-tagged ORF (FL) only gave rise to an extremely low level of polypeptide product (Supplementary Figure S4). The lack of OCC-1 polypeptide, in some extent, may due to the high GC-content of OCC-1 5′UTR and the highly stable hairpin structure around the initial codon, which would lower the translational efficiency dramatically (38). In addition, a novel noncoding OCC-1 splice variant (OCC-1D) was also discovered in CRC, in which a 60-nucleotide RNA fragment containing the initial codon of OCC-1 ORF was spliced out (39). Thus, we supposed that OCC-1 RNA has noncoding function independent of its polypeptide product in CRC cells. In fact, overexpression of the frameshift-mutated full-length OCC-1 RNA (FS^+) with disrupted ORF in OCC-1 knockdown cells have similar suppressive effect as the full-length RNA (FL^+), but overexpression of OCC-1 ORF, which produces the polypeptide, has no obvious effect on cell growth (Figure 3). Furthermore, we also found that the OCC-1 exerts its function primarily by binding to HuR through its relative long AU-rich 3′UTR, which contains numerous *in vivo* HuR-binding motifs. Taken together, these observations indicate that OCC-1 functions, at least in CRC cells, primarily as a lncRNA.

The oncogenic effect of HuR is mainly attributed to its binding to and stabilization of cancer-associated mRNAs in the cytoplasm (26). As HuR is predominantly nuclear, the translocation of HuR into the cytoplasm, which is regulated by a nuclear-cytoplasmic shuttling sequence (40) and several nuclear import proteins (41), may important for its oncogenic function. In addition, the phosphorylation of HuR, which is mediated by several cancer-related kinases such as Chk2, PKCα and PKCδ, also influence its cytoplasmic localization and RNA binding property (42,43). Recently, OIP5-AS1, a lncRNA that represses HeLa cell proliferation, was found to regulate HuR function by serving as a sponge that competes for HuR from its target mRNAs (18). Here, we revealed that OCC-1 regulates the level of HuR protein through promoting its ubiquitination and degradation at post-translational level. Our results introduced an additional mechanism by which HuR is regulated in cancer cells.

To date, a few of lncRNAs have also been found to regulate the post-translational modifications of their binding proteins. NKILA, a lncRNA that suppresses breast cancer metastasis, forms stable complex with NF-κB/IκB and directly masks the phosphorylation motifs of IκB, thereby inhibiting IκB phosphorylation and subsequent NF-κB activation (44). In contrast, lnc-DC, a lncRNA which is required for human dendritic cell differentiation and function, prevents the transcription factor STAT3 from dephosphorylation by SHP1, a protein tyrosine phosphatase for STAT3, which in turn maintains STAT3 activity (45). In the case of Lnc-DC-STAT3 interaction, the binding of Lnc-DC attenuated the association between STAT3 and the phosphatase SHP1, thereby preserving the phosphorylated state of STAT3. Thus, the binding of lncRNAs could influence the availability of the modification sites or the association between the post-translational modification enzymes and the target proteins. In present study, we found that OCC-1

promotes HuR ubiquitination by enhancing its binding to it ubiquitin E3 ligase β-TrCP1 (Figure 6), which could recognize HuR and catalyze its ubiquitination. As the binding of β-TrCP1 to OCC-1 was not detected in the RNA pulldown assay (data not shown), we proposed that the binding of OCC-1 to HuR could make it more accessible to β-TrCP1. Recently, another lncRNA, lncRNA-LET, has also been found to promote the ubiquitination of another RBP, nuclear factor 90 (NF90)(46). Although the mechanism for lncRNA-LET in regulating ubiquitination is still unknown, our study suggests that this could be a common mechanism for lncRNAs in control of protein levels at post-translational level.

OCC-1 regulates the levels of a large number of mRNAs through modulating HuR in CRC. GO analysis revealed that the OCC-1-repressed genes are mainly enriched for the regulators of gene expression that function at post-transcriptional and translational level (25). Meanwhile, many of these OCC-1-repressed genes have been found to directly involve in cancer cell growth, such as HNRNPA1 (47) and HNRNPK (48), which encode splicing factors, EIF3M (49) and EIF4E (50), which encode eukaryotic translation initiation factors, and mitotic division-associated genes MAD2L1 (51) and NEK2 (52). We reasoned that the upregulation of these genes is directly responsible for the increased cell growth in OCC-1 knockdown cells. Until now, only one type of lncRNAs, half-STAU1-binding site RNAs (1/2-sbsRNAs), was reported to have the ability to regulate the levels of a large number of mRNAs at post-transcriptional level (53). 1/2-sbsRNAs contain Alu repeat elements which duplex with the mRNAs that have homogenous Alu elements in their 3′UTRs and lead the mRNAs to staufen 1-mediated mRNA decay. In this study, we revealed that OCC-1 can also regulate a large number of mRNAs through modulating HuR ubiquitination and degradation, which also demonstrates the extensive regulatory effects of lncRNAs on mRNA homeostasis.

In summary, here we found that OCC-1 suppresses cell growth through inhibition of G0 to G1 and G1 to S phase cell cycle transitions as a lncRNA in CRC. OCC-1 binds to HuR and promotes its degradation, thereby reducing the levels of HuR protein and its target mRNAs, including these mRNAs directly associated with cancer cell growth. Our study suggests that lncRNA can regulate the levels of a large number of mRNAs at post-transcriptional level through modulating RBP ubiquitination and degradation, and that modulation of protein ubiquitination could be a common mechanism for lncRNA in control of protein level at post-translational level.

DATA AVAILABILITY

Microarray data are deposited at the Gene Expression Omnibus database with the accession Number GSE108816.

SUPPLEMENTARY DATA

Supplementary Data are available at NAR Online.

FUNDING

National Key R&D Program of China [2017YFA0504300]; National Natural Science Foundation of China [31771441, 81490752, 31371325, 31671347, 31000579, 30971634]; Doctoral Programs Foundation of the Ministry of Education, China [20130181130010]. Funding for open access charge: National Key R&D Program of China.
Conflict of interest statement. None declared.

REFERENCES

1. Derrien,T., Johnson,R., Bussotti,G., Tanzer,A., Djebali,S., Tilgner,H., Guernec,G., Martin,D., Merkel,A., Knowles,D.G. *et al.* (2012) The GENCODE v7 catalog of human long noncoding RNAs: analysis of their gene structure, evolution, and expression. *Genome Res.*, **22**, 1775–1789.
2. Fatica,A. and Bozzoni,I. (2014) Long non-coding RNAs: new players in cell differentiation and development. *Nat. Rev. Genet.*, **15**, 7–21.
3. Huarte,M. (2015) The emerging role of lncRNAs in cancer. *Nat. Med.*, **21**, 1253–1261.
4. Zhao,J., Sun,B.K., Erwin,J.A., Song,J.J. and Lee,J.T. (2008) Polycomb proteins targeted by a short repeat RNA to the mouse X chromosome. *Science*, **322**, 750–756.
5. Gupta,R.A., Shah,N., Wang,K.C., Kim,J., Horlings,H.M., Wong,D.J., Tsai,M.C., Hung,T., Argani,P., Rinn,J.L. *et al.* (2010) Long non-coding RNA HOTAIR reprograms chromatin state to promote cancer metastasis. *Nature*, **464**, 1071–1076.
6. Wang,K.C., Yang,Y.W., Liu,B., Sanyal,A., Corces-Zimmerman,R., Chen,Y., Lajoie,B.R., Protacio,A., Flynn,R.A., Gupta,R.A. *et al.* (2011) A long noncoding RNA maintains active chromatin to coordinate homeotic gene expression. *Nature*, **472**, 120–124.
7. Song,X., Sun,Y. and Garen,A. (2005) Roles of PSF protein and VL30 RNA in reversible gene regulation. *Proc. Natl. Acad. Sci. U.S.A.*, **102**, 12189–12193.
8. Ng,S.Y., Bogu,G.K., Soh,B.S. and Stanton,L.W. (2013) The long noncoding RNA RMST interacts with SOX2 to regulate neurogenesis. *Mol. Cell*, **51**, 349–359.
9. Xing,Z., Lin,A., Li,C., Liang,K., Wang,S., Liu,Y., Park,P.K., Qin,L., Wei,Y., Hawke,D.H. *et al.* (2014) lncRNA directs cooperative epigenetic regulation downstream of chemokine signals. *Cell*, **159**, 1110–1125.
10. Clemson,C.M., Hutchinson,J.N., Sara,S.A., Ensminger,A.W., Fox,A.H., Chess,A. and Lawrence,J.B. (2009) An architectural role for a nuclear noncoding RNA: NEAT1 RNA is essential for the structure of paraspeckles. *Mol. Cell*, **33**, 717–726.
11. Tsai,M.C., Manor,O., Wan,Y., Mosammaparast,N., Wang,J.K., Lan,F., Shi,Y., Segal,E. and Chang,H.Y. (2010) Long noncoding RNA as modular scaffold of histone modification complexes. *Science*, **329**, 689–693.
12. Kino,T., Hurt,D.E., Ichijo,T., Nader,N. and Chrousos,G.P. (2010) Noncoding RNA gas5 is a growth arrest- and starvation-associated repressor of the glucocorticoid receptor. *Sci. Signal*, **3**, ra8.
13. Di Ruscio,A., Ebralidze,A.K., Benoukraf,T., Amabile,G., Goff,L.A., Terragni,J., Figueroa,M.E., De Figueiredo Pontes,L.L., Alberich-Jorda,M., Zhang,P. *et al.* (2013) DNMT1-interacting RNAs block gene-specific DNA methylation. *Nature*, **503**, 371–376.
14. Ji,Q., Zhang,L., Liu,X., Zhou,L., Wang,W., Han,Z., Sui,H., Tang,Y., Wang,Y., Liu,N. *et al.* (2014) Long non-coding RNA MALAT1 promotes tumour growth and metastasis in colorectal cancer through binding to SFPQ and releasing oncogene PTBP2 from SFPQ/PTBP2 complex. *Br. J. Cancer*, **111**, 736–748.
15. Poliseno,L., Salmena,L., Zhang,J., Carver,B., Haveman,W.J. and Pandolfi,P.P. (2010) A coding-independent function of gene and pseudogene mRNAs regulates tumour biology. *Nature*, **465**, 1033–1038.
16. Hansen,T.B., Jensen,T.I., Clausen,B.H., Bramsen,J.B., Finsen,B., Damgaard,C.K. and Kjems,J. (2013) Natural RNA circles function as efficient microRNA sponges. *Nature*, **495**, 384–388.
17. Memczak,S., Jens,M., Elefsinioti,A., Torti,F., Krueger,J., Rybak,A., Maier,L., Mackowiak,S.D., Gregersen,L.H., Munschauer,M. *et al.*

(2013) Circular RNAs are a large class of animal RNAs with regulatory potency. *Nature*, **495**, 333–338.
18. Kim,J., Abdelmohsen,K., Yang,X., De,S., Grammatikakis,I., Noh,J.H. and Gorospe,M. (2016) LncRNA OIP5-AS1/cyrano sponges RNA-binding protein HuR. *Nucleic Acids Res.*, **44**, 2378–2392.
19. Yan,X., Hu,Z., Feng,Y., Hu,X., Yuan,J., Zhao,S.D., Zhang,Y., Yang,L., Shan,W., He,Q. *et al.* (2015) Comprehensive genomic characterization of long non-coding RNAs across human cancers. *Cancer Cell*, **28**, 529–540.
20. Mourtada-Maarabouni,M., Pickard,M.R., Hedge,V.L., Farzaneh,F. and Williams,G.T. (2009) GAS5, a non-protein-coding RNA, controls apoptosis and is downregulated in breast cancer. *Oncogene*, **28**, 195–208.
21. Prensner,J.R., Iyer,M.K., Sahu,A., Asangani,I.A., Cao,Q., Patel,L., Vergara,I.A., Davicioni,E., Erho,N., Ghadessi,M. *et al.* (2013) The long noncoding RNA SChLAP1 promotes aggressive prostate cancer and antagonizes the SWI/SNF complex. *Nat. Genet.*, **45**, 1392–1398.
22. Glisovic,T., Bachorik,J.L., Yong,J. and Dreyfuss,G. (2008) RNA-binding proteins and post-transcriptional gene regulation. *FEBS Lett.*, **582**, 1977–1986.
23. Kim,M.Y., Hur,J. and Jeong,S. (2009) Emerging roles of RNA and RNA-binding protein network in cancer cells. *BMB Rep.*, **42**, 125–130.
24. Lopez de Silanes,I., Zhan,M., Lal,A., Yang,X. and Gorospe,M. (2004) Identification of a target RNA motif for RNA-binding protein HuR. *Proc. Natl. Acad. Sci. U.S.A.*, **101**, 2987–2992.
25. Lebedeva,S., Jens,M., Theil,K., Schwanhausser,B., Selbach,M., Landthaler,M. and Rajewsky,N. (2011) Transcriptome-wide analysis of regulatory interactions of the RNA-binding protein HuR. *Mol. Cell*, **43**, 340–352.
26. Abdelmohsen,K. and Gorospe,M. (2010) Posttranscriptional regulation of cancer traits by HuR. *Wiley Interdiscip. Rev.: RNA*, **1**, 214–229.
27. Denkert,C., Koch,I., von Keyserlingk,N., Noske,A., Niesporek,S., Dietel,M. and Weichert,W. (2006) Expression of the ELAV-like protein HuR in human colon cancer: association with tumor stage and cyclooxygenase-2. *Modern. Pathol.*, **19**, 1261–1269.
28. Lopez de Silanes,I., Fan,J., Yang,X., Zonderman,A.B., Potapova,O., Pizer,E.S. and Gorospe,M. (2003) Role of the RNA-binding protein HuR in colon carcinogenesis. *Oncogene*, **22**, 7146–7154.
29. Abdelmohsen,K., Srikantan,S., Yang,X., Lal,A., Kim,H.H., Kuwano,Y., Galban,S., Becker,K.G., Kamara,D., de Cabo,R. *et al.* (2009) Ubiquitin-mediated proteolysis of HuR by heat shock. *EMBO J.*, **28**, 1271–1282.
30. Chu,P.C., Chuang,H.C., Kulp,S.K. and Chen,C.S. (2012) The mRNA-stabilizing factor HuR protein is targeted by beta-TrCP protein for degradation in response to glycolysis inhibition. *J. Biol. Chem.*, **287**, 43639–43650.
31. Kikuchi,K., Fukuda,M., Ito,T., Inoue,M., Yokoi,T., Chiku,S., Mitsuyama,T., Asai,K., Hirose,T. and Aizawa,Y. (2009) Transcripts of unknown function in multiple-signaling pathways involved in human stem cell differentiation. *Nucleic Acids Res.*, **37**, 4987–5000.
32. Pibouin,L., Villaudy,J., Ferbus,D., Muleris,M., Prosperi,M.T., Remvikos,Y. and Goubin,G. (2002) Cloning of the mRNA of overexpression in colon carcinoma-1: a sequence overexpressed in a subset of colon carcinomas. *Cancer Genet. Cytogenet.*, **133**, 55–60.
33. Franken,N.A., Rodermond,H.M., Stap,J., Haveman,J. and van Bree,C. (2006) Clonogenic assay of cells in vitro. *Nat. Protoc.*, **1**, 2315–2319.
34. Irizarry,R.A., Hobbs,B., Collin,F., Beazer-Barclay,Y.D., Antonellis,K.J., Scherf,U. and Speed,T.P. (2003) Exploration, normalization, and summaries of high density oligonucleotide array probe level data. *Biostatistics*, **4**, 249–264.
35. Yu,G., Wang,L.G., Han,Y. and He,Q.Y. (2012) clusterProfiler: an R package for comparing biological themes among gene clusters. *OMICS*, **16**, 284–287.
36. Yu,G., Li,F., Qin,Y., Bo,X., Wu,Y. and Wang,S. (2010) GOSemSim: an R package for measuring semantic similarity among GO terms and gene products. *Bioinformatics*, **26**, 976–978.
37. Mukherjee,N., Corcoran,D.L., Nusbaum,J.D., Reid,D.W., Georgiev,S., Hafner,M., Ascano,M. Jr, Tuschl,T., Ohler,U. and Keene,J.D. (2011) Integrative regulatory mapping indicates that the RNA-binding protein HuR couples pre-mRNA processing and mRNA stability. *Mol. Cell*, **43**, 327–339.
38. Babendure,J.R., Babendure,J.L., Ding,J.H. and Tsien,R.Y. (2006) Control of mammalian translation by mRNA structure near caps. *RNA*, **12**, 851–861.
39. Najafi,H., Soltani,B.M., Dokanehiifard,S., Nasiri,S. and Mowla,S.J. (2017) Alternative splicing of the OCC-1 gene generates three splice variants and a novel exonic microRNA, which regulate the Wnt signaling pathway. *RNA*, **23**, 70–85.
40. Fan,X.C. and Steitz,J.A. (1998) HNS, a nuclear-cytoplasmic shuttling sequence in HuR. *Proc. Natl. Acad. Sci. U.S.A.*, **95**, 15293–15298.
41. Rebane,A., Aab,A. and Steitz,J.A. (2004) Transportins 1 and 2 are redundant nuclear import factors for hnRNP A1 and HuR. *RNA*, **10**, 590–599.
42. Abdelmohsen,K., Pullmann,R. Jr, Lal,A., Kim,H.H., Galban,S., Yang,X., Blethrow,J.D., Walker,M., Shubert,J., Gillespie,D.A. *et al.* (2007) Phosphorylation of HuR by Chk2 regulates SIRT1 expression. *Mol. Cell*, **25**, 543–557.
43. Doller,A., Huwiler,A., Muller,R., Radeke,H.H., Pfeilschifter,J. and Eberhardt,W. (2007) Protein kinase C alpha-dependent phosphorylation of the mRNA-stabilizing factor HuR: implications for posttranscriptional regulation of cyclooxygenase-2. *Mol. Biol. Cell*, **18**, 2137–2148.
44. Liu,B., Sun,L., Liu,Q., Gong,C., Yao,Y., Lv,X., Lin,L., Yao,H., Su,F., Li,D. *et al.* (2015) A cytoplasmic NF-kappaB interacting long noncoding RNA blocks IkappaB phosphorylation and suppresses breast cancer metastasis. *Cancer Cell*, **27**, 370–381.
45. Wang,P., Xue,Y., Han,Y., Lin,L., Wu,C., Xu,S., Jiang,Z., Xu,J., Liu,Q. and Cao,X. (2014) The STAT3-binding long noncoding RNA lnc-DC controls human dendritic cell differentiation. *Science*, **344**, 310–313.
46. Yang,F., Huo,X.S., Yuan,S.X., Zhang,L., Zhou,W.P., Wang,F. and Sun,S.H. (2013) Repression of the long noncoding RNA-LET by histone deacetylase 3 contributes to hypoxia-mediated metastasis. *Mol. Cell*, **49**, 1083–1096.
47. Liu,X., Zhou,Y., Lou,Y. and Zhong,H. (2016) Knockdown of HNRNPA1 inhibits lung adenocarcinoma cell proliferation through cell cycle arrest at G0/G1 phase. *Gene*, **576**, 791–797.
48. Sugimasa,H., Taniue,K., Kurimoto,A., Takeda,Y., Kawasaki,Y. and Akiyama,T. (2015) Heterogeneous nuclear ribonucleoprotein K upregulates the kinetochore complex component NUF2 and promotes the tumorigenicity of colon cancer cells. *Biochem. Biophys. Res. Commun.*, **459**, 29–35.
49. Goh,S.H., Hong,S.H., Hong,S.H., Lee,B.C., Ju,M.H., Jeong,J.S., Cho,Y.R., Kim,I.H. and Lee,Y.S. (2011) eIF3m expression influences the regulation of tumorigenesis-related genes in human colon cancer. *Oncogene*, **30**, 398–409.
50. Wan,J., Shi,F., Xu,Z. and Zhao,M. (2015) Knockdown of eIF4E suppresses cell proliferation, invasion and enhances cisplatin cytotoxicity in human ovarian cancer cells. *Int. J. Oncol.*, **47**, 2217–2225.
51. Chen,F., Liu,S., Zhou,Y., Shen,H. and Zuo,X. (2016) Mad2 overexpression is associated with high cell proliferation and reduced disease-free survival in primary gastrointestinal diffuse large B-cell lymphoma. *Hematology*, **21**, 399–403.
52. Wu,S.M., Lin,S.L., Lee,K.Y., Chuang,H.C., Feng,P.H., Cheng,W.L., Liao,C.J., Chi,H.C., Lin,Y.H., Tsai,C.Y. *et al.* (2017) Hepatoma cell functions modulated by NEK2 are associated with liver cancer progression. *Int. J. Cancer*, **140**, 1581–1596.
53. Gong,C. and Maquat,L.E. (2011) lncRNAs transactivate STAU1-mediated mRNA decay by duplexing with 3′ UTRs via Alu elements. *Nature*, **470**, 284–288.